

## Measurement of the atomic lifetime of Kr II $5p^4D_{7/2}^{\circ}$ and Xe II $6p^4D_{5/2}^{\circ}$ using the cascade-photon-coincidence technique

R. E. Mitchell, S. D. Rosner, T. J. Scholl, and R. A. Holt

*Physics Department, University of Western Ontario, London, Ontario, Canada N6A 3K7*

(Received 21 October 1991; revised manuscript received 10 December 1991)

A high-efficiency cascade-photon-coincidence lifetime-measuring apparatus has been used to study the  $5d^4F_{9/2} \rightarrow 5p^4D_{7/2}^{\circ} \rightarrow 5s^4P_{5/2}$  cascade in Kr II and the  $6d^4F_{7/2} \rightarrow 6p^4D_{5/2}^{\circ} \rightarrow 6s^4P_{3/2}$  cascade in Xe II. A neutral atomic beam was excited and ionized by electron impact, and the spontaneously emitted photons were collected by an ellipsoidal mirror and detected by fast photomultipliers provided with narrow-band interference filters. The spectrum of time delays was acquired by a time-to-amplitude converter and multichannel pulse-height analyzer. The lifetime of the Kr II  $5p^4D_{7/2}^{\circ}$  state was found to be  $7.004 \pm 0.053$  ns. This is in agreement with two previous high-precision measurements and represents an improvement in precision by a factor of 3.6. The Xe II  $6p^4D_{5/2}^{\circ}$  lifetime was found to be  $9.494 \pm 0.067$  ns. This result agrees with several measurements of lower accuracy, but is in clear disagreement with two previous measurements claiming high precision, which disagree with each other as well.

PACS number(s): 32.70.Fw

### I. INTRODUCTION

Radiative lifetimes of atoms are of interest in such fields as plasma physics [1], laser physics [2], astrophysics, and solar physics [3–5], as well as fundamental physics [6]. The older techniques involving measurements of the intensity of emission of a plasma, the absorption of a gas cell, or the measurement of anomalous dispersion by the Hook method have been reviewed by Wiese [7]. The more recent beam-foil, beam-gas, beam-laser, level-crossing, pulsed-electron-excitation, and cascade-photon-coincidence (CPC) methods have been reviewed by Corney [8] and by Imhof and Read [9]. The pulsed-electron excitation and early beam-foil results sometimes had large systematic errors from undesired cascading; more recently, the arbitrarily normalized decay curve (ANDC) method [10] has greatly improved the situation. The beam-laser and CPC techniques should be inherently free of this problem, although they require a high degree of detector selectivity. It is disturbing therefore to find measurements of this type in the literature that claim accuracies of better than 3% and yet that differ by nearly 20%.

In the present work, we have measured two atomic lifetimes of interest in ion laser physics, one of which involves just such a discrepancy. Our result for the lifetime of the  $5p^4D_{7/2}^{\circ}$  level of Kr II, which is the lower state of a lasing transition [11], is in complete agreement with two earlier  $\approx 3\%$  measurements [12, 13], which agreed with each other to their stated accuracies. This measurement represents an improvement by a factor of 3.6. In the case of the  $5p^4D_{7/2}^{\circ}$  level of Xe II, which is the upper state of one of the most prominent Xe laser lines as well as the lower state of a weaker line [11], there are previous results [12, 13] that claim 1.4% and 2.9% accuracy, yet that differ by 18%. Our measurement has an accuracy of 0.7%, and disagrees with both previous values.

### II. APPARATUS AND TECHNIQUE

The CPC technique makes use of a cascade, in which a highly excited atom relaxes through a series of less excited states by spontaneous emission of photons. Photons from a transition whose lower level is the atomic state of interest are selected using a narrow-bandwidth optical filter. They are detected with a high-gain photomultiplier, whose fast timing output signal starts a time-to-amplitude converter (TAC). A second photomultiplier detects photons from a transition whose upper level is the atomic state of interest, and its fast timing output stops the TAC. The atoms are continuously and nonselectively excited to all possible energy levels by electron impact or other means. The time interval or delay between the detection of a start and a stop photon is a measure of the length of time the atom has spent in the intermediate state of the cascade. The probability for the atom to remain in this state for a time  $t$  is given by  $\exp(-t/\tau)$ , where  $\tau$  is the mean lifetime of the intermediate state. A histogram of observed time delays is thus a direct measurement of the decay probability density distribution, from which  $\tau$  can be extracted. In addition to this exponential time-delay spectrum of “true” coincidences, there is always in practice a background of random coincidences arising from photons emitted by different atoms or from dark counts, resulting in a nearly uniform number of counts added to each channel. This technique has been used extensively in nuclear physics; its use for atomic lifetime determinations was originally demonstrated by Brannen *et al.* [14].

Figure 1 shows a schematic diagram of our experimental apparatus. Atoms were ionized and excited by electron impact at the intersection of a beam of neutral atoms and an electron beam; this crossing is located at the first focal point of an ellipsoidal mirror. Due to their low thermal velocity of less than 300 m/s and lifetimes on the or-

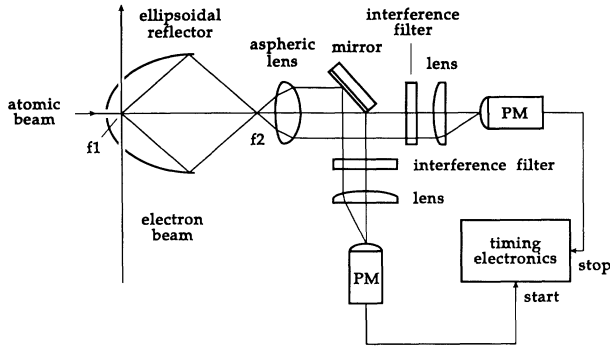


FIG. 1. Schematic diagram of the apparatus for cascade-photon-coincidence measurements of atomic lifetimes. The light source is formed at the intersection of the electron and atomic beams. The focal points of the ellipsoidal reflector are denoted by  $f_1$  and  $f_2$ .

der of  $10^{-8}$  s, the atoms decay to lower states, with the emission of light, well before leaving the source region at  $f_1$ . The photons emitted in this region were focused by the ellipsoid at the second focal point  $f_2$ . The solid angle subtended by the ellipsoidal reflector is  $0.78 \times 4\pi$  sr and the reflectivity of the rhodium overcoating is 0.77 in the visible region of the spectrum. An antireflection-coated aspheric condensing lens collimated the light from the source image at  $f_2$ . Half of the light beam leaving the lens was reflected at  $90^\circ$  by a 50-mm-square aluminum mirror with a dielectric overcoating. The direct and reflected beams passed through narrow-bandwidth optical filters and were then focused onto the photocathodes of their respective photomultipliers by antireflection-coated lenses.

The source of electrons was a commercially available BaO-cathode electron gun located in a separate vacuum chamber; this allowed the electron gun to be differentially pumped and minimized the amount of background light from the cathode. The electron-optical system consisted of two sets of steering plates followed by a second einzel lens and a beam-defining aperture. The electron beam current was typically  $100 \mu\text{A}$ , with a beam diameter of 2 mm at  $f_1$ . To eliminate the effects of the earth's magnetic field, the apparatus was located in a near-zero magnetic field region provided by rectangular Helmholtz coils.

The atom beam was supplied by a large gas cell at  $10^{-3}$  Torr from which gas effused into the main chamber through a 1 mm  $\times$  10 mm beam-defining aperture

located 3 cm from  $f_1$ . The background gas pressure in the main chamber was approximately  $10^{-6}$  Torr. The use of an atomic beam effectively eliminates the problems of collisional deexcitation and radiation trapping [15]. The latter was not a problem in this experiment in any event, because all of the states involved were short-lived excited states of the *ionic* species, and thus had extremely low population densities. Collisional deexcitation, on the other hand, is often an important source of systematic error in lifetime measurements performed in a cell, because the cross sections for several processes, such as charge exchange, are extremely large for an ion colliding with its parent neutral [16, 17]. For this reason, we chose to use a beam rather than a cell of atomic vapor.

The choice of an optimum source intensity has been discussed by several authors [9, 18]. At very low intensities the signal-to-background ratio is high because the true coincidences vary linearly with source intensity while the random background coincidences vary quadratically; however, the rate of data collection goes to zero as the source intensity is reduced. The signal-to-noise ratio increases in a nonlinear way with increasing source intensity, suggesting that high intensities are desirable; however, various systematic effects in the counting electronics become significant, especially when the probability of "multistop events" becomes non-negligible [19]. For this reason, the source intensity was generally chosen to yield a signal-to-background ratio on the order of 1.

An important factor in CPC measurements is the choice of narrow-bandwidth optical filters, which must isolate the cascade of interest from two types of interfering cascades. One type is another cascade in which the photons from the first and second transition happen to fall within the bandpasses of the start and stop detectors, respectively. The second process is the "reverse" cascade in which the photons of the *second* transition provide events to the start channel and photons from the *first* transition provide stop events. These reverse cascades contribute decay curves that decrease exponentially to the left of zero time delay.

For the experiments described here, two-cavity all-dielectric filters with a full-width at half maximum (FWHM) bandwidth between 2.5 and 3.0 nm were used. The transmission outside the pass band was 0.01% and the filters were blocked to wavelengths from the x ray to  $1.2 \mu\text{m}$ . Tables I and II show the cascades used in our experiments, the wavelengths of the transitions, and the filter characteristics. The cascade selected for our krypton lifetime was different from that studied by Mohamed,

TABLE I. Cascades, transition wavelengths, and interference filter characteristics used in the Kr II  $5p^4D_{7/2}^o$  lifetime measurement.

	Start channel	Stop channel
Transition	$5d^4F_{9/2} \rightarrow 5p^4D_{7/2}^o$	$5p^4D_{7/2}^o \rightarrow 5s^4P_{5/2}$
Transition wavelength (nm)	378.313	435.547
Filter wavelength (nm)	379.0	436.2
Filter bandwidth FWHM (nm)	2.8	3.0
Filter peak transmission	32%	64%

TABLE II. Cascades, transition wavelengths, and interference filter characteristics used in the Xe II  $6p\ ^4D_{5/2}^o$  lifetime measurement.

	Start channel	Stop channel
Transition	$6d\ ^4F_{7/2} \rightarrow 6p\ ^4D_{5/2}^o$	$6p\ ^4D_{5/2}^o \rightarrow 6s\ ^4P_{3/2}$
Transition wavelength (nm)	433.052	541.915
Filter wavelength (nm)	433.35	542.5
Filter bandwidth FWHM (nm)	2.9	2.5
Filter peak transmission	50%	73%

King, and Read [12] in order to eliminate the effects of the two reverse cascades that contributed to their spectra. The cascade for our xenon measurement corresponds to the one used by Mohamed, King, and Read [12]. In our experiment, however, interference filters with a FWHM bandwidth narrower by a factor of more than 2 were chosen to obtain better isolation of the cascade under study.

A schematic diagram of the data-acquisition circuitry is shown in Fig. 2. The start and stop photons were detected by Amperex XP2020Q fast linear-focused 12-stage photomultipliers that had been specifically selected for low dark-count rates. The “linear” dynode voltage divider chain recommended by Philips [20] for this application was used. Each photomultiplier output was sent to an Ortec 9301 fast-timing preamplifier followed by an Ortec 473A discriminator which can operate in either the leading-edge or the constant-fraction mode. The discriminators provided fast-timing pulses to the start and stop inputs of an Ortec 467 time-to-amplitude converter. In order that the TAC operate in its most linear region and to allow the random background to be measured, a fixed time delay was inserted in the stop channel using an Ortec model 425A nanosecond delay cable box. The TAC output pulses were measured by a Tracor-Northern 1750 multichannel pulse-height ana-

lyzer (PHA). The data stored in the PHA are thus in the form of a histogram of the number of coincidences versus time delay.

### III. EQUIPMENT CALIBRATION

The absolute time calibration of the TAC-PHA system was accomplished using an Ortec 462 time calibrator. The crystal time base of the Ortec 462 was checked against two other stable crystal clocks. Then, two widely separated peaks that spanned the PHA spectrum were generated, and the “dispersion” feature of the 462 was used to spread each peak over several PHA channels. The centers of these peaks were located using a nonlinear least-squares fit of the peak to a Gaussian function. The average channel width was found to be  $332.62 \pm 0.33$  ps. The channel width was found to be independent of the rate at which the time-delay spectrum was acquired and independent of normal laboratory temperature variations.

The differential nonlinearity of the conversion of time-delay intervals into channel numbers by the TAC-PHA system is a measure of the uniformity of channel widths. It is defined as  $\pm \frac{1}{2}(W_{\max} - W_{\min})/W_{\text{av}}$  where  $W_{\max}$ ,  $W_{\min}$ , and  $W_{\text{av}}$  are the maximum, minimum, and average channel widths, respectively. It was measured using a Čerenkov source to supply random start signals and a clocked pulse generator to supply stop signals. The time interval between a start and stop signal is thus a random value and there is also no correlation between starting times of successive measurements. The channel widths  $W_i$  of the TAC-PHA timing system are then proportional to the number of counts registered in the  $i$ th channel. The rate of coincidence events during this test was about 1 count/s in each channel. The time required to accumulate  $4 \times 10^5$  counts per channel was approximately 110 h. The resulting spectrum indicated no structure that could be identified above statistical counting error.

The prompt response curve of the detectors and the electronics was measured using a  $100\text{-}\mu\text{Ci}\ ^{90}\text{Sr-}^{90}\text{Y}$  Čerenkov source, which emits  $\beta$  particles of 0.55 and 2.27 MeV maximum energy. It was enclosed in a stainless-steel capsule with a  $50\text{-}\mu\text{m}$  aluminum window, encased in a cylindrical Lucite Čerenkov medium, and placed at the first focal point of the ellipsoidal reflector. The source produced an average of 6 to 24 photons per  $\beta$  particle that fell within the bandwidth of the broadest light filters used to measure the prompt response curve. The experimental conditions were such that the probability of more than one simultaneous photon striking one of

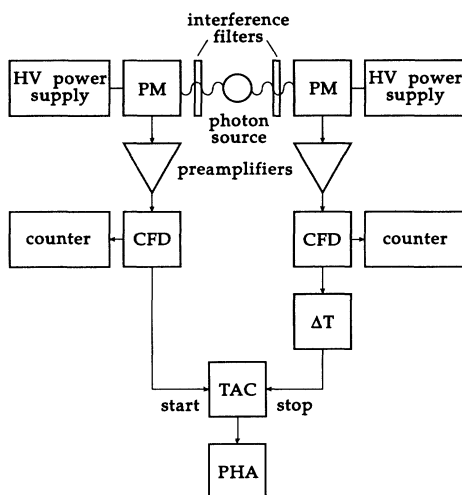


FIG. 2. Schematic of the electronics showing the detection and timing circuitry. PM, photomultiplier; HV, high voltage; CFD, constant-fraction discriminator;  $\Delta T$ , fixed time delay; TAC, time-to-amplitude converter; PHA, pulse-height analyzer.

the photocathodes was negligible.

A very detailed study of the prompt response curve was undertaken once it became apparent that this would be the dominant systematic error in the experiment. As can be seen from Fig. 3, the prompt response curve was not a simple Gaussian. In addition to a large main peak centered about zero time delay, two pairs of much smaller symmetrically located satellite peaks were also evident. These satellites were not due to ringing [21] in the photomultiplier output because the discriminator responds to the *first* part of the signal to cross its threshold, and then has an internal dead time of 65 ns. In addition, the count rates of the experiment were low enough that the probability that the first peak of a photomultiplier event would be processed was essentially unity.

Similar prompt response curves have been observed by Bebelaar [22], who attributed the outermost small peaks to backscattering of primary electrons that impinge on the first dynode of the photomultiplier and are elastically or inelastically scattered without producing secondary electrons. If an electron is scattered in the correct direction (by the first dynode or another part of the photomultiplier structure), it can nearly reach the photocathode and return to strike the dynode a second time. The time it takes the electron to complete this round trip is about twice the transit time between the photocathode and the first dynode. For the XP2020Q photomultiplier operated at 2600 V the round-trip transit time has been calculated [22] to be 11.6 ns. In this experiment, where the operating voltage of the photomultiplier was approximately 2 kV, the outermost peaks were separated from the main peak by  $15.1 \pm 0.1$  ns. The additional peaks very close to the main peak are thought to be due to photoelectrons that hit elements of the photomultiplier tube structure closer to the photocathode.

If we assume that Bebelaar's explanation is correct, then the peak to the left (right) side of the main prompt response peak is due to backscattering in the start (stop)

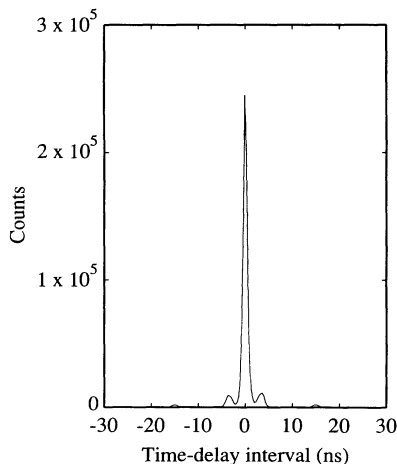


FIG. 3. The prompt response function, or instrumental time resolution, obtained with the discriminators in the constant-fraction mode, with 36-nm interference filters spanning the wavelengths of the Kr II cascade.

channel photomultiplier, respectively. To test this hypothesis, we increased the operating voltage of either the start or the stop channel photomultiplier from 2 to 2.4 kV to alter the transit time of the backscattered electrons and found that the correct individual satellite peaks furthest from the main peak were shifted closer to the zero-time-delay channel by an amount in agreement with the expected  $V^{1/2}$  law. We therefore believe that the complex nature of the prompt response curve is most likely due to backscattered photoelectrons.

The shape of the prompt curve was also found to depend on the wavelength of the optical filters and on the operational mode (leading-edge or constant-fraction) of the discriminators. The dependence of the response curve on the photon wavelength can be attributed to the initial velocity of the photoelectron. For these reasons, the prompt response curve was measured under the conditions of each of the lifetime measurements.

#### IV. KRYPTON MEASUREMENT AND RESULTS

##### A. Data acquisition and analysis

The krypton lifetime measurement was taken over the course of 300 h. Figure 4 shows the CPC spectrum obtained. The peak channel had about 15000 counts, corresponding to a statistical uncertainty of 0.8%. The prompt response curve was measured over 212 h. The peak channel had about 250 000 counts, with an uncertainty of 0.2%; thus, the prompt response curve is known to a higher degree of statistical accuracy than the lifetime spectrum. This is important because we are fitting the lifetime spectrum to an analytic function convolved with a measured instrumental response function, which can thus add additional uncertainty and systematic errors.

The analysis is complicated by the fact that the expected curve even in the case of an infinitely narrow prompt response function is not simply an exponential plus a constant random background. The functional form of the time-delay spectrum in this ideal case is [19, 23]

$$N(t) = \left[ A e^{-t/\tau} H(t - t_0) + B \right] e^{-R_{\text{stop}} t}, \quad (1)$$

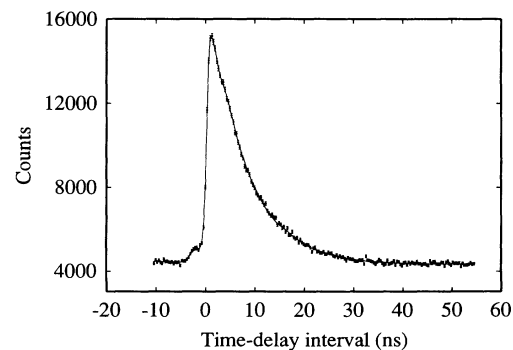


FIG. 4. The time-delay spectrum for the Kr II  $5p^4 D_{7/2}^{\circ}$  lifetime measurement, with the least-squares fit to the convolution of the ideal spectrum of Eq. (1) with the measured prompt response curve.

where  $R_{\text{stop}}$  is the stop photon counting rate,  $A$  is the amplitude of the exponential curve,  $B$  is the random background,  $t_0$  is the prompt time corresponding to zero time delay, and  $H(t - t_0)$  is a Heaviside unit step function. A TAC spectrum is not actually a histogram of time delays, because only the *first* stop signal following a given start signal is recorded. This introduces a bias against detecting long delays when the count rate is high enough to have a significant chance for two or more stop events to occur within the TAC time range. The factor outside the brackets represents the Poisson-distribution probability that no stop event has occurred between times 0 and  $t$ . It can be neglected for our typical stop count rates of  $10^4$  counts/s. At higher count rates the spectrum can be corrected by multiplying the raw data by  $e^{R_{\text{stop}}t}$ .

The experimental TAC-PHA spectrum was fitted to the convolution of the ideal spectrum given by Eq. (1) with the measured instrumental response function. The lifetime of the atomic state was determined using nonlinear least-squares fitting in which the four parameters  $A$ ,  $B$ ,  $t_0$ , and  $\tau$  in Eq. (1) were varied to minimize  $\chi^2$ . In calculating  $\chi^2$ , we did not include the uncertainty introduced by the numerical convolution with an imperfectly known prompt response curve. Thus the  $\chi^2$  probabilities we obtain are conservative estimates.

### B. Systematic errors

To study the effect of the wavelength dependence of the prompt response curve on the lifetime, the same CPC spectrum was analyzed using two different prompt response curves. The first was taken with 36-nm filters in front of the photomultipliers and the second was measured without any filters whatsoever. The fitted lifetime changed by 1.4%, and the  $\chi^2$  probability decreased from 5% to  $1 \times 10^{-6}$ . The uncertainty introduced by the measured response curve would certainly be much less than the 1.4% change using the “wide-open” prompt curve; as a reasonable estimate of the uncertainty introduced by our imperfect knowledge of the prompt response curve we have chosen 0.5%. This and the other error estimates are listed in Table III.

The region of the CPC spectrum analyzed was selected according to two criteria. The first was that the spectrum contain a reasonable segment of the background on either side of the channel corresponding to zero time delay. The data to the left of zero determine the background pa-

rameter independently; if only data to the right of zero are included in the fit, the correlation between the background and the lifetime parameters becomes larger and they are not as well determined. The second criterion was that the analysis region be free of contributions from the TAC-PHA system noise and nonlinearity close to the low end of the spectrum. The change in the lifetime measurement due to changes in the region of analysis consistent with these two criteria was 0.1%.

The dependence of the fitted lifetime on the stop rate was negligible in these experiments. This dependence was tested by varying the stop rate used to correct the data in the fitting routine from  $3 \times 10^3$  to  $5 \times 10^4$  counts/s. The fitted lifetime changed by  $\approx 0.1\%$  and the  $\chi^2$  probability did not change significantly. As the stop event count rate for this measurement was 7400 counts/s, the effect of the correction was not significant.

There is a small spurious contribution to the CPC spectra due to cosmic radiation, which causes simultaneous events in both photomultipliers even when their shutters are closed. A cosmic-ray background spectrum taken over the course of 250 h had 90 counts registered in the peak channel. Over the 300-h data accumulation time for the Kr II measurement, the expected cosmic-ray contribution to the prompt channel was approximately 110 counts; this is about the same size as the uncertainty due to counting statistics. The cosmic-ray contribution occurs in the transition region from constant background on the left-hand side of time zero to the exponential decay curve plus constant background on the right; this region contributes significantly to the  $\chi^2$  value. The measured cosmic-ray spectrum was scaled to the collection time for the lifetime measurement and then subtracted directly from the raw data. A reasonable estimate of the uncertainty in the lifetime due to this correction is 0.1%. This estimate is calculated as the change in the lifetime from the value obtained with the subtraction of the correct cosmic-ray peak to that obtained when only 75% of the peak is subtracted, thus assuming a conservative 25% uncertainty in our knowledge of the cosmic-ray contribution. When no correction at all was made for cosmic rays, the fitted lifetime changed by 0.5%.

The uncertainty introduced by the differential nonlinearity of the TAC-PHA system was estimated as follows. Because no systematic deviations from uniform channel widths were found, there was no justification for making a correction to the channel widths. To test this assumption, such a correction was made, using a technique described by Turner [24]. A change in the lifetime of less than 0.1% was observed; thus, as a reasonable estimate of the uncertainty due to differential nonlinearity we have chosen 0.1%.

From the foregoing discussion, it is apparent that the only necessary correction to the data before fitting was the subtraction of the cosmic-ray contribution. The lifetime of the  $5p^4D_{7/2}^o$  state of Kr II obtained from the least-squares fit was  $7.004 \pm 0.038$  ns, where the error included only the statistical uncertainty of the fit. The reduced  $\chi^2$  of the fit shown in Fig. 4 is 1.16 per degree of freedom. The  $\chi^2$  probability is 6.7%, indicating an excellent fit. The final uncertainty in the lifetime measurement was

TABLE III. Contribution of sources of error to the total uncertainty in the lifetime measurements.

Source of error	Contribution (%)
Statistical uncertainty of fit	0.5
Knowledge of prompt response curve	0.5
Cosmic ray events	0.1
Absolute time calibration	0.1
Differential nonlinearity of TAC-PHA	0.1
Region of spectrum analyzed	0.1
Stop rate effect	0.1

obtained by adding in quadrature the statistical uncertainty and the systematic error estimates listed in Table III. The overall uncertainty is 0.8%, corresponding to 0.053 ns.

### C. Discussion

A comparison of our Kr II results with previous lifetime measurements and calculations is presented in Table IV. The pulsed-electron excitation technique was used by Delgado, Campos, and Sánchez del Rio [25], Donnelly, Kindlmann, and Bennett [26], Blagoev [27], and Fonseca and Campos [28]. These groups used threshold-energy electrons in an attempt to excite only the state of interest. The excitation took place in a gas cell where the pressure-dependent effect of collisional deexcitation was present. This effect was corrected for by a linear extrapolation of the data to zero pressure; it is not clear, however, that this is a valid assumption. LeMond and Head [29] made no attempt to eliminate cascading from their beam-gas measurement, and Schade *et al.* [30] carried out their pulsed-laser-excitation experiment in a discharge cell.

The high-precision beam-laser and CPC results agree with our measurement within experimental error. The slightly higher value of Mohamed, King, and Read [12] may be due to undesired contributions from several other known cascades. Two reverse cascades contributed an

exponentially decreasing spectrum to the left of the time zero; their effect on the spectrum was corrected for in the data analysis. In addition, however, there were small but probably non-negligible contributions from two forward cascades that were unaccounted for. For this reason, we chose a different cascade and used interference filters with a narrower 3.0-nm FWHM bandwidth. The measurement of Mohamed, King, and Read [12] represents the weighted mean of five independent lifetime measurements. Each spectrum had about 3300 counts in the peak channel, corresponding to a large statistical uncertainty of 1.7%. The value of  $\chi^2$  was then small and its probability large, indicating a good fit. However, this may be misleading, because the large statistical error in a single spectrum could mask systematic errors, which were treated as negligible. A more stringent test of the fit would be obtained by summing the five spectra.

The systematic errors of the beam-laser technique have been discussed by Ward *et al.* [13]. The accuracy of the ion beam velocity calibration was given as 1%. The systematic error due to the variation in the step length was 1%, and the variation in the detected efficiency along the ion beam was quoted as 0.5%. For both the krypton and xenon measurements considered here, a tail fitting routine was used that did not include the substantial amount of data near the earliest decay times. The uncertainty in the lifetime measurement due to the statistical fit of the

TABLE IV. Summary of measured and calculated values of the lifetime of the Kr II  $5p^4D_{7/2}^o$  state. IC, intermediate coupling; HFS, Hartree-Fock-Slater; BD, Bates-Damgaard; PEE, pulsed-electron excitation; CPC, cascade-photon coincidence; BL, beam-laser; BG, beam-gas, PLE, pulsed-laser excitation.

Source	Method	Lifetime (ns)
Theory		
Marantz, Rudko, and Tang <sup>a</sup>	IC-HFS	6.8±1.4
Koozekanani and Trusty <sup>b</sup>	IC-HFS	6.08
El Sherbini <sup>c</sup>	IC-BD	5.6
Spector and Garpman <sup>d</sup>	IC-HFS	6.1
Helbig <sup>e</sup>	LS-BD	7.13
Fonseca and Campos <sup>f</sup>	LS-BD	6.9
Experiment		
Delgado, Campos, and Sánchez del Rio <sup>g</sup>	PEE	8.5±0.3
Donnelly, Kindlmann, and Bennett <sup>h</sup>	PEE	7.70±0.15
Mohamed, King, and Read <sup>i</sup>	CPC	7.22±0.22
Blagoev <sup>j</sup>	PEE	8.8±0.8
Fonseca and Campos <sup>f</sup>	PEE	7.0±0.7
Ward <i>et al.</i> <sup>k</sup>	BL	7.04±0.19
LeMond and Head <sup>l</sup>	BG	8.0±0.5
Schade <i>et al.</i> <sup>m</sup>	PLE	7.2±0.5
This work	CPC	7.004±0.053

<sup>a</sup>Reference [33].

<sup>b</sup>Reference [34].

<sup>c</sup>Reference [35].

<sup>d</sup>Reference [36].

<sup>e</sup>Reference [31].

<sup>f</sup>Reference [28].

<sup>g</sup>Reference [25].

<sup>h</sup>Reference [26].

<sup>i</sup>Reference [12].

<sup>j</sup>Reference [27].

<sup>k</sup>Reference [13].

<sup>l</sup>Reference [29].

<sup>m</sup>Reference [30].

data was stated as varying between 0.9% and 2.6%. This represented the largest single contribution to the uncertainty in the measurement.

The results of theoretical calculations have been included in Table IV as well. Helbig [31] and Fonseca and Campos [28] used  $LS$ -coupling wave functions together with radial functions from the Coulomb approximation of Bates and Damgaard [32]; both are within 2% of our experimental result. Marantz, Rudko, and Tang [33], Koozekanani and Trusty [34], El Sherbini [35], and Spector and Garpman [36] used intermediate-coupling wave functions with the coefficients of the  $LS$  basis functions adjusted by least-squares fitting to reproduce the experimentally known energy levels. The radial functions were evaluated by either the Hartree-Fock-Slater method [37] or, in the case of El Sherbini [35], the Coulomb approximation. These differ from our measured value by amounts ranging from 3% to 20%. No uncertainties were included in most cases, although Marantz [33] stated an accuracy of 20%.

## V. XENON MEASUREMENT

### A. Data acquisition and results

The CPC spectrum for the Xe II  $6p^4D_{5/2}^o$  lifetime measurement was accumulated over 70 h. The electron current was  $90 \mu\text{A}$ ; this relatively large current allowed the gas density to be reduced from the previous krypton measurement while maintaining a high rate of coincidence events. The “true” coincidence rate was  $\approx 0.3$  counts/s, and the stop rate was about 7 200 counts/s. The uncertainty due to counting statistics in the peak channel was 0.8%. A prompt response curve was accumulated over 385 h, with 36-nm-wide optical filters. This gave 42 000 counts in the peak channel, for an uncertainty of 0.5%, which was thus of the same order of magnitude as the statistical uncertainty in the lifetime spectrum itself. When it became apparent that our knowledge of the instrumental response was the most significant contribution to the error budget, we decided to remeasure the prompt curve with the actual interference filters used in the lifetime measurement. This measurement lasted for 2 573 h and yielded 23 000 counts in the peak channel.

A cosmic-ray correction was made to both the lifetime spectrum and the prompt response spectrum. The scaled cosmic-ray contribution to the peak channel corresponded to one-fifth of the statistical uncertainty in the peak channel of the lifetime spectrum. For completeness, the lifetime data were also corrected for the stop rate. Using the 36-nm prompt response curve, the lifetime of the  $6p^4D_{5/2}^o$  state was found to be  $9.553 \pm 0.043$  ns (statistical uncertainty only). The reduced  $\chi^2$  was 1.27. Using the prompt curve obtained with the actual interference filters of the lifetime experiment, the fitted value of the lifetime changed to  $9.494 \pm 0.043$  ns and the reduced  $\chi^2$  improved slightly to 1.24. This fit is shown in Fig. 5. The change of  $-0.6 \pm 0.6\%$  justifies the estimate for the uncertainty due to the instrumental response function we arrived at in Sec. IV B. We have chosen to

retain this quantity in our systematic error budget for the Xe II lifetime, even though we are using the prompt curve measured with the actual filters, because the reduced  $\chi^2$  of 1.24 is higher than expected for 439 degrees of freedom (probability 0.04%). This reflects the fact that there are still some systematic differences between the fitted curve and the data in the region very close to time zero. It is reasonable to suppose that these are caused by the slight changes in the optical system introduced by the Čerenkov source, with its Lucite medium and metal parts. It should, however, be emphasized that the true  $\chi^2$  is lower, because our estimate of  $\chi^2$  does not take into account the uncertainty introduced by using a *measured* instrumental response function. With the systematic error estimates from Sec. IV B included, the final result is  $9.494 \pm 0.067$  ns.

Despite great care in the search for interfering cascades and in the choice of interference filters, we must consider the possibility that another cascade is contaminating the lifetime spectrum. In our measurement, the amount of data accumulated in the time-delay spectrum was large enough that the uncertainty in the lifetime due to the statistical fit was less than the contributions from sources of systematic error, thus allowing us to probe the single-exponential shape of the curve in detail. We carried out a numerical simulation of the effect of an admixture of a second cascade on the least-squares fit. The only way in which we were able to change the lifetime by 10% without producing extremely large  $\chi^2$  values was by mixing in an interfering cascade whose amplitude was of comparable magnitude to the one under study. Since the latter is formed by two of the most intense lines in the xenon spectrum, it is highly improbable that the two high-intensity spectral lines of the hypothesized interfering cascade would have been completely overlooked in the literature.

### B. Discussion

A summary of the measurements of the  $6p^4D_{5/2}^o$  level of Xe II is given in Table V. The two intensity measurement methods [31, 43] relied on an estimate of the

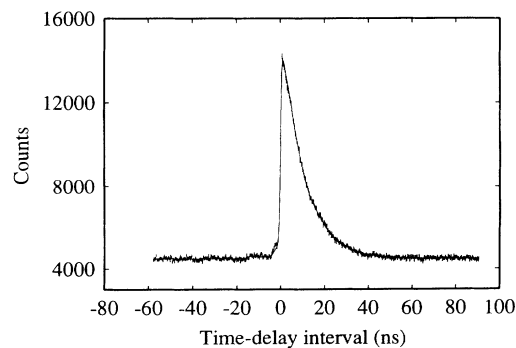


FIG. 5. The time-delay spectrum for the Xe II  $6p^4D_{5/2}^o$  lifetime measurement, with the least-squares fit to the convolution of the ideal spectrum of Eq. (1) with the measured prompt response curve.

number of fluorescing atoms in the source region, making the absolute measurement unreliable. Three different groups measured the lifetime of this state using the pulsed-electron-excitation technique. Two of the groups, Allen, Jones, and Schofield [39] and Jiménez, Campos, and Sánchez del Río [40] used excitation electron energies above the threshold level required to populate the excited atomic state, thus very likely leading to cascading. The measurement by Donnelly, Kindlmann, and Bennett [38] used threshold energy electrons to excite the atoms in the gas cell. While this can reduce the problem of unwanted cascading, this experiment and the other two experiments using this technique are subject to pressure-dependent effects.

Measurements by the beam-foil technique were performed by Andersen, Madson, and Sørensen [41] and Coetzer and van der Westhuizen [42]. The former group used a low-energy ion beam to reduce the effects of cascading and spectral line blending. The latter group used a high-energy beam, and the measurement was more likely to be subject to these effects. Of the measurements that state an accuracy of 10% or better, the results of Donnelly, Kindlmann, and Bennett [38] and Andersen, Madson, and Sørensen [41] agree with our result within experimental error. It should be noted that in these experiments some care was taken to reduce undesirable effects inherent in their respective experimental techniques.

Of all of these measurements, three claim accuracies of 3% or better: those of Ward *et al.* [13], Mohamed, King, and Read [12], and the present work. No two of these agree within experimental error. There are several reasons why we believe our measurement to be correct. The first is spectral resolution. One of the key elements of the CPC technique is that the cascade of interest must be isolated so that no other correlated photons can contribute coincidence counts to the time-delay spectrum. Our experiment employed interference filters with bandwidths of 2.9 and 2.5 nm, compared to 7 and 6 nm in the measurement of Mohamed, King, and Read [12].

Another potentially significant difference between the two cascade experiments was the gas pressure in the observation region. Mohamed, King, and Read used  $5 \times 10^{-3}$  Torr in their Xe II experiment (compared to  $3 \times 10^{-3}$  Torr for their Kr II measurements), whereas our xenon atoms were emerging as a beam under collision-free conditions into a region with a background pressure of  $10^{-6}$  Torr. Although the total collisional deexcitation cross section for the  $6p^4D_{5/2}^o$  state is not known, it is well known that various collision cross sections for xenon ions with neutral xenon atoms are very large at thermal energies [16, 17]. If we make the assumption that the  $6p$  level deexcitation cross section is ten times the  $10^{-14}$  cm<sup>2</sup> ground-state charge-exchange cross section [16, 17], we arrive at a very rough estimate of a 1% effect on the life-

TABLE V. Summary of measured and calculated values of the lifetime of the Xe II  $6p^4D_{5/2}^o$  state. BD, Bates-Damgaard; IC, intermediate coupling; PP, parametric potential; HFS, Hartree-Fock-Slater; HFRC, Hartree-Fock with relativistic corrections; PEE, pulsed-electron excitation; BF, beam-foil; CPC, cascade-photon coincidence; BL, beam-laser.

Source	Method	Lifetime (ns)
Theory		
Allen, Jones, and Schofield <sup>a</sup>	LS-BD	11
Jiménez, Campos, and Sánchez del Río <sup>b</sup>	LS-BD	8.8
El Sherbini <sup>c</sup>	IC-PP	11.3
Garpman and Spector <sup>d</sup>	IC-HFS	9.3
Helbig <sup>e</sup>	LS-BD	8.86
Coetzer and van der Westhuizen <sup>f</sup>	LS-BD	8.64
Hansen <sup>g</sup>	IC-HFRC	7.01
Experiment		
Allen, Jones, and Schofield <sup>a</sup>	PEE	11±5
Andersen, Madson, and Sørensen <sup>h</sup>	BF	10.5±1.0
Donnelly, Kindlmann, and Bennett <sup>i</sup>	PEE	9.9±0.5
Jiménez, Campos, and Sánchez del Río <sup>b</sup>	PEE	11.5±1.5
Mohamed, King, and Read <sup>j</sup>	CPC	8.70±0.12
Coetzer and van der Westhuizen <sup>k</sup>	BF	11.0±1.9
Ward <i>et al.</i> <sup>l</sup>	BL	7.30±0.21
This work	CPC	9.494±0.067

<sup>a</sup>Reference [39].

<sup>b</sup>Reference [40].

<sup>c</sup>Reference [45].

<sup>d</sup>Reference [46].

<sup>e</sup>Reference [31].

<sup>f</sup>Reference [42].

<sup>g</sup>Reference [44].

<sup>h</sup>Reference [41].

<sup>i</sup>Reference [38].

<sup>j</sup>Reference [12].

<sup>k</sup>Reference [42].

<sup>l</sup>Reference [13].

time; this is still too small to explain the 8% discrepancy. Furthermore, Mohamed, King, and Read state [12] that "increasing the target gas pressure by an order of magnitude did not produce any change in the measured lifetime," although they do not indicate whether this check was carried out for each state they studied. Because our measurements were carried out under atomic-beam conditions, we have more confidence that collisional deexcitation was completely negligible.

Unlike Mohamed, King, and Read, who claim that all systematic errors were negligible, we have thoroughly investigated the systematic errors quantitatively. The large-wavelength dependence of the prompt response curve, which can cause a change in the measured lifetime by 1.4%, has been studied extensively. Also included in our data analysis are corrections for the cosmic-ray contribution. Although this effect was reduced by the wider separation of the photomultiplier photocathodes in the experiment of Mohamed, King, and Read, it could still have contributed a nonnegligible effect.

Some questions concerning the beam-laser experiment of Ward *et al.* have recently been raised by Hansen and Persson [44] as a result of their extensive revised analysis of the Xe II spectrum. In footnote 57 of their paper, they point out that the  $6p^4D_{5/2}^o$  level is not the upper state of the Xe II line at 680.574 nm in the more recent analysis and thus could not have been excited by laser radiation at that wavelength, as claimed. (They also point out in the same footnote that this wavelength could not have been produced by rhodamine 560 dye, as stated in Table I of Ref. [13]; however, we assume that this was simply a misprint for rhodamine 640.) Thus it appears that there is a real possibility that Ward *et al.* actually made a measurement of a different excited level of Xe II.

There are also some minor problems in the beam-laser measurement. The systematic errors were stated as 1% for the variation in the step length between adjacent channels of the intensity measurement and 0.5% for the variation in the detection efficiency along the ion beam path. However, no correction for these effects was made in the data analysis. The uncertainty of the accelerating voltage of the ion beam of the beam-laser method was quoted as 1%. As in most beam-foil experiments, this experiment did not measure the velocity of the ions directly during the experiment, when it might have varied. Scattered light is usually a serious concern of the beam-laser technique; this was, however, stated not to be a problem for the two measurements in question. A large portion of the spectrum in the vicinity of  $t_0$  was not

used. It is in this region that a great deal can be learned about systematic errors. This was amply demonstrated in our own work with the discovery of the wavelength dependence of the prompt response curve when we included this region, which would otherwise have been rejected in a simple tail-fitting analysis.

As in the Kr II case, there is no clear evidence for the superiority of the more sophisticated calculational techniques used by El Sherbini [45], Garpman and Spector [46], and Hansen and Persson [44] over the Coulomb approximation with  $LS$  coupling. The result of Hansen and Persson [44] is the only one that seems to favor the measurement of Ward *et al.*; however, the authors summarize all of their calculations by stating, "Compared to the experimental lifetimes our calculated values are systematically shorter by 1–2 ns." The spread of calculated values is somewhat greater than for krypton, perhaps indicating the increased difficulty of including relativistic effects such as spin-orbit mixing and the resultant lack of any good approximate coupling scheme for this heavy ion. A reasonable estimate of the reliability of the calculations would be no better than 15–20%.

## VI. CONCLUSIONS

Our measurement of the  $5p^4D_{7/2}^o$  state of Kr II agrees with previous results claiming high accuracy. This measurement improves the precision with which the lifetime is known by a factor of 3.6.

The discrepancy in the precision lifetime measurements of the  $6p^4D_{5/2}^o$  level of Xe II in this work and that of Ward *et al.* [13] and Mohamed, King, and Read [12] remains unresolved. What makes the problem interesting is the excellent agreement of the three results for Kr II by the same groups. Further measurements of this type by techniques capable of high precision may provide enough information to resolve this kind of discrepancy that is unfortunately not unique to this case.

## ACKNOWLEDGMENTS

We gratefully acknowledge the financial support of the Natural Sciences and Engineering Research Council of Canada, the Academic Development Fund of the University of Western Ontario, and the Centre of Excellence in Molecular and Interfacial Dynamics (CEMAID). We thank J. Girash for valuable assistance during the construction of the apparatus and during data acquisition.

[1] H. B. Gilbody, *Adv. At. Mol. Phys.* **15**, 293 (1979).  
 [2] W. B. Bridges, in *Methods of Experimental Physics: Quantum Electronics*, edited by C. L. Tang (Academic, New York, 1979), Vol. 15A, p. 31.  
 [3] P. L. Smith, *Nucl. Instrum. Methods* **110**, 395 (1973).  
 [4] J. J. Wynne, *Phys. Today*, **36** (11), 52 (1983).  
 [5] N. Grevesse, *Phys. Scr.* **T8**, 49 (1984).  
 [6] R. Crossley, *Phys. Scr.* **T8**, 117 (1984).

[7] W. L. Wiese, in *Methods of Experimental Physics*, edited by L. Marton (Academic, New York, 1968), Vol. 7A, p. 117.  
 [8] A. Corney, in *Advances in Electronics and Electron Physics*, edited by L. Marton (Academic, New York, 1970), Vol. 29, p. 115.  
 [9] R. E. Imhof and F. H. Read, *Rep. Prog. Phys.* **40**, 1 (1977).

- [10] L. J. Curtis, H. G. Berry, and J. Bromander, *Phys. Lett.* **34A**, 169 (1971).
- [11] W. B. Bridges and A. N. Chester, *IEEE J. Quantum Electron.* **QE-1**, 66 (1965).
- [12] K. A. Mohamed, G. G. King, and F. H. Read, *J. Phys. B* **10**, 1835 (1977).
- [13] L. Ward, A. Wännström, A. Arnesen, R. Hallin, and O. Vogel, *Phys. Scr.* **31**, 149 (1985).
- [14] E. Brannen, F. R. Hunt, R. H. Adlington, and R. W. Nicholls, *Nature* **175**, 810 (1955).
- [15] A. C. G. Mitchell and M. W. Zemansky, *Resonance Radiation and Excited Atoms* (Cambridge University Press, New York, 1971).
- [16] A. Dalgarno, *Philos. Trans. R. Soc. London. Ser. A* **250**, 426 (1958).
- [17] H. Helm, *J. Phys. B* **9**, 2931 (1976).
- [18] R. A. Holt and F. M. Pipkin, *Phys. Rev. A* **9**, 581 (1974).
- [19] R. A. Lundy, *Phys. Rev.* **125**, 1686 (1962).
- [20] Philips Data Handbook T9: Electron Tubes (Philips Export B.V., Eindhoven, The Netherlands, 1985).
- [21] B. H. Candy, *Rev. Sci. Instrum.* **56**, 183 (1985).
- [22] D. Beelaar, *Rev. Sci. Instrum.* **57**, 1116 (1986).
- [23] D. W. Gidley, Ph.D. thesis, University of Michigan, 1979.
- [24] C. E. Turner, Jr., *Nucl. Instrum. Methods* **87**, 45 (1970).
- [25] A. Delgado, J. Campos, and C. Sánchez del Rio, *Z. Phys. A* **257**, 9 (1972).
- [26] K. E. Donnelly, P. J. Kindlmann, and W. R. Bennett, Jr., *J. Opt. Soc. Am.* **65**, 1359 (1975).
- [27] K. B. Blagoev, *J. Phys. B* **14**, 4743 (1981).
- [28] V. Fonseca and J. Campos, *J. Phys. B* **15**, 2349 (1982).
- [29] J. E. LeMond and C. E. Head, *Nucl. Instrum. Methods B* **24**, 309 (1987).
- [30] W. Schade, Z. W. Stryla, V. Helbig, and G. Langhans, *Phys. Scr.* **39**, 246 (1989).
- [31] V. Helbig, Ph.D. thesis, Kiel University, Germany, 1978.
- [32] D. R. Bates and A. Damgaard, *Philos. Trans. R. Soc. London Ser. A* **242**, 101 (1949).
- [33] H. Marantz, R. I. Rudko, and C. L. Tang, *IEEE J. Quantum Electron.* **QE-5**, 38 (1969).
- [34] S. H. Koozekanani and G. L. Trusty, *J. Opt. Soc. Am.* **59**, 1281 (1969).
- [35] Th. M. El Sherbini, *Z. Phys. A* **276**, 325 (1976).
- [36] N. Spector and S. Garpman, *J. Opt. Soc. Am.* **67**, 155 (1977).
- [37] F. Herman and S. Skillman, *Atomic Structure Calculations* (Prentice-Hall, Englewood Cliffs, NJ, 1963).
- [38] K. E. Donnelly, P. J. Kindlmann, and W. R. Bennett, Jr., *J. Opt. Soc. Am.* **63**, 1438 (1973); *IEEE J. Quantum Electron.* **QE-10**, 848 (1974).
- [39] L. Allen, D. G. C. Jones, and D. G. Schofield, *J. Opt. Soc. Am.* **59**, 842 (1969).
- [40] E. Jiménez, J. Campos, and C. Sánchez del Rio, *J. Opt. Soc. Am.* **64**, 1009 (1974).
- [41] T. Andersen, O. H. Madsen, and G. Sørensen, *Phys. Scr.* **6**, 125 (1972).
- [42] F. J. Coetzer and P. van der Westhuizen, *Z. Phys. A* **292**, 369 (1979).
- [43] M. H. Miller, R. A. Roig, R. D. Bengtson, *Phys. Rev. A* **8**, 480 (1973).
- [44] J. E. Hansen and W. Persson, *Phys. Scr.* **36**, 602 (1987).
- [45] Th. M. El Sherbini, *Z. Phys. A* **275**, 1 (1975).
- [46] S. Garpman and N. Spector, *J. Opt. Soc. Am.* **66**, 904 (1976).